Scientia Iranica B (2013) 20 (3), 467–476

Sharif University of Technology

Scientia Iranica

Transactions B: Mechanical Engineering

www.sciencedirect.com

Hall and ion-slip effect on MHD boundary layer flow of a micro polar fluid past a wedge

Z. Uddin [a,b,*], **M. Kumar** [c]

[a] *ITM University, Gurgaon, Haryana, 122017, India*

[b] *Université de Lille Nord de France, F-59000, Lille, UVHC, TEMPO/DF2T, F-59313 Valenciennes, France*

[c] *G.B. Pant University of Agriculture and Technology, Pantnagar, Uttarakhand 263145, India*

Received 4 July 2011; revised 29 November 2012; accepted 21 January 2013

KEYWORDS

Micropolar fluids;
Hall current;
Ion slip;
Wedge;
Applied numerical methods.

Abstract This paper deals with the influence of Hall and ion slip effects on the magneto-hydrodynamic flow of a micropolar fluid past a non-conducting wedge. The analysis has been made by assuming that the fluid is viscous, incompressible and electrically conducting. The partial differential equations governing the flow and heat transfer are converted into highly non-linear ordinary differential equations by using the similarity transformations. These equations are then solved numerically. The effects of various parameters involved in the problem have been studied with the help of graphs and numerical values of skin friction coefficients and Nusselt number are presented in tabular form. Favorable comparison with previously published work on various special cases of the problem has been made. Results show that the local skin friction coefficient due to translational motion increases with the angle of the wedge and Hall effect parameter; hence heat transfer rate increases with these parameters. The result gets reversed with a increase in material, ion slip and magnetic field parameters.

1. Introduction

The study of magneto-micropolar fluid flow in a slip-flow regime with Hall and ion slip currents is very important considering its vast applications to many engineering problems such as power generators, magneto-hydrodynamic accelerators, refrigeration coils, transmission lines, electric transformers and heating elements. Also, many industrial applications involve fluids as a working medium. In such applications unclean fluids (i.e. clean fluid+ interspersed particles) are very common and clean fluid is an exception. Therefore the classical Navier Stokes equation is not suitable for modelling such types of problem.

Eringen [1,2] proposed a theory of micropolar fluids taking into account the inertial characteristics of the substructure particles, which are allowed to undergo rotation. The concept of micropolar fluids deals with a class of fluids that exhibit certain microscopic effects arising from the local structure and micro motions of fluid elements. These fluids contain dilute suspensions of rigid macromolecules with individual motions that support stress and body moments influenced by spin inertia. The interaction of the macro velocity field and micro rotation field can be described through new material constants in addition to those of classical Newtonian fluids. Eringen's micro polar fluid model includes the classical Navier–Stokes equations for a viscous and incompressible fluid as a special case. These micropolar fluids are suitable in modeling for studying the flow of colloidal fluids, polymers, lubricants, cerebro fluids, liquid crystals, animal blood, real fluids with suspensions and ferro fluids etc., for which the classical Navier–Stokes theory is inadequate. The equations governing the flow of a micropolar fluid involve a microrotation vector and a gyration parameter in addition to the classical vector field. The micropolar fluid theory requires an additional transport equation representing the principle of conservation of local angular momentum. An extensive review of the theory and applications of micropolar fluids can be found in [3,4].

In consideration of these things, various researchers worked on micropolar fluids. Jena and Mathur [5] studied the laminar

* Corresponding author at: ITM University, Gurgaon, Haryana, 122017, India. Tel.: +91 9873782027.

E-mail address: ziya_dd@rediffmail.com (Z. Uddin).

Peer review under responsibility of Sharif University of Technology.

Production and hosting by Elsevier

doi:10.1016/j.scient.2013.02.013

Nomenclature

$\overrightarrow{J}$	*Current density vector*
Ec	*Eckert number*
$\overrightarrow{E}$	*Electric field intensity*
$\overrightarrow{H}$	*Magnetic field intensity*
$\overrightarrow{B}$	*Magnetic Induction vector*
$\overrightarrow{N}$	*Microrotation vector normal to xy-plane*
$\overrightarrow{V}$	*Translational velocity vector*
C_{fx}	*Local skin friction coefficient*
C_{fz}	*Local skin friction coefficient*
C_p	*Specific heat at constant pressure*
I	*Inertial parameter*
K	*Material parameter*
k	*Thermal conductivity of the fluid*
Nu	*Local Nusselt number*
p	*Pressure*
Pr	*Prandtl number*
Re	*Reynolds number*
T	*Temperature*
u, v, w	*Components of velocity along x, y and z axes respectively*

Greek symbols

ψ	Steam function
Θ	Dissipation function
Ω	*Wedge angle*
j	*Micro-inertia*
β	*Hartree pressure gradient parameter*
β_e	*Hall effect parameter*
β_i	*Ion slip parameter*
γ	Spin gradient viscosity
η	Non-dimensional distance
κ	Vortex viscosity
μ	Dynamic viscosity
ρ	Density of the fluid
σ	Electrical conductivity
τ_e	*Electron mean free time*
τ_i	*Ion mean free time*
ω_e	*Electron cyclotron frequency*
ω_i	*Ion cyclotron frequency*

Superscript

$'$	*Derivative with respect to* η

free convection boundary layer flow of a thermomicropolar fluid past a non-isothermal vertical plate and found the similarity solution for the flow. A numerical study of micropolar convective heat and mass transfer in a non-Darcy porous regime with Soret and Dufour diffusion effects has been done by Beg et al. [6]. Norfifah [7] investigated the steady magneto-hydrodynamic stagnation point flow of a micropolar fluid past a vertical surface under different temperature conditions. Recently, Pal and Chatterjee [8] developed a numerical model to examine the combined effects of Soret and Dufour on mixed convection magneto-hydrodynamic heat and mass transfer in micropolar fluid saturated Darcian porous medium in the presence of thermal radiation, non uniform heat source and ohmic dissipation.

Also, magneto-hydrodynamic (MHD) boundary layer flow over wedge shaped bodies is very common in many thermal engineering applications such as geothermal systems, crude oil extraction, ground water pollution, thermal insulation, heat exchangers and the storage of nuclear waste etc. Lin and Lin [9] found the similarity solutions for laminar forced convection heat transfer from wedges to fluids of any Prandtl number. Kim [10,11] have considered the steady boundary layer flow of a micropolar fluid past a wedge with constant surface temperature and constant surface heat flux, respectively. The similarity variables found by Falkner and Skan [12] were employed to reduce the governing partial differential equations to ordinary differential equations. Kafoussias and Nanousis [13] investigated the magneto-hydrodynamic laminar boundary layer flow over a permeable wedge immersed in a Newtonain fluid. The study of magneto-hydrodynamic forced convection flow adjacent to a non-isothermal wedge is done by Yih [14]. This work is extended by Chamka et al. [15]. They considered the thermal radiation effects on magneto-hydrodynamic forced convection flow adjacent to a non-isothermal wedge in the presence of a heat source or sink. Paramjeet et al. [16] considered time dependent free stream velocity and gave a mathematical model for the unsteady mixed convection flow of an incompressible viscous fluid over a vertical wedge with constant suction/injection and analyzed the behavior of the flow. The steady two-dimensional laminar forced convection flow and heat transfer of a viscous, incompressible, electrically conducting and heat generating fluid past a permeable wedge embedded in a non-Darcy high porosity ambient medium with uniform surface heat flux is studied by Rashad and Bakier [17].

In a magneto-hydrodynamic device using weakly ionized gases Hall and ion-slip effects appear as the ratio of magnetic field strength to gas density. A boundary layer analysis is used to study the effects of Hall and ion-slip currents on steady magneto-micropolar, incompressible, electrically conducting and viscous fluid over a horizontal plate by Seddeek and Abdelmeguid [18]. Hazem [19,20] investigated the Hall effect on Couette flow with heat transfer of a dusty conducting fluid by assuming uniform suction/injection and temperature dependent physical properties, respectively. Ibrahim [21] found the analytic solution of magneto-hydrodynamic mixed convection heat and mass transfer over an isothermal, inclined permeable stretching plate immersed in a uniform porous medium in the presence of chemical reaction, internal heating, Dufour effect and Hall effects. Elgazery [22] also studied the Hall and ion slip effects on magneto-hydrodynamic flow along with temperature dependent viscosity and thermal diffusivity.

Recently, Ishak et al. [23] studied the steady laminar magneto-hydrodynamic boundary layer flow past a wedge with constant surface heat flux immersed in an incompressible micropolar fluid in the presence of a variable magnetic field. They ignored, the Hall term and ion slip conditions in applying Ohm's law as it has no marked effect for small and moderate values of the magnetic field. However, the current trend for the application of magneto-hydrodynamics is towards a strong magnetic field, so the influence of electromagnetic fields is noticeable. Under these conditions, the Hall current is important and it has a marked effect on the magnitude and direction of current density and consequently on the magnetic force. Therefore the objective of the present paper is to study the magneto-hydrodynamic (MHD) flow past a wedge by considering viscous dissipation, Joule heating, and Hall and ion-slip effects.

2. Formulation

A steady viscous, incompressible, electrically conducting and micro-polar fluid flowing past a non conducting wedge

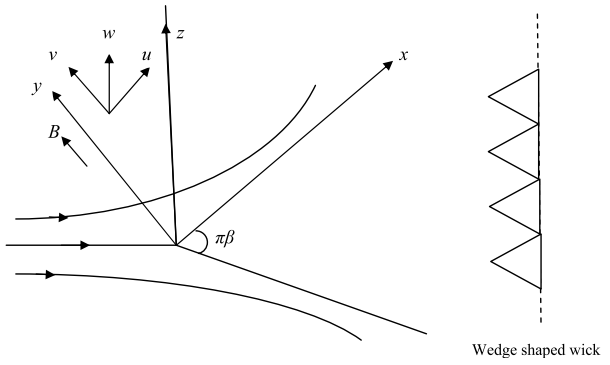

Figure 1: Physical Model and coordinate system Wedge shaped wick.

is considered. This flow can be considered as the flow past a triangular or wedge shaped wick inside the heat pipe or heat exchanger. The physical model and coordinate system of the problem are shown in Figure 1.

The authors use rectangular Cartesian coordinates (x, y, z), in which x, y and z are the distances measured along the wedge, normal to the surface of the wedge and along the leading edge of the wedge respectively. A strong magnetic filed $B(x)$ is applied along the y-axis and the fluid is considered electrically conducting. Thus, Hall and ion-slip currents affect the flow. This effect give rise to force in the direction perpendicular to the magnetic field, which induces a cross flow in that direction, i.e. z-direction. For the steady, incompressible, magneto-hydrodynamic flow of micropolar fluid with generalized Ohm's law, including Hall and ion-slip (see Sutton [24]) and under the assumption that the fluid is non-magnetic, and neglecting the thermoelectric effect the equations in vector form are:

Conservation of mass:

$$div\,\vec{V} = 0. \tag{1}$$

Conservation of translational momentum:

$$\rho(\vec{V}.\vec{\nabla})\vec{V} = -(\vec{\nabla}p) + (2\mu+\kappa)\vec{\nabla}(\vec{\nabla}.\vec{V}) - (\mu+\kappa)\vec{\nabla}\times\left(\vec{\nabla}\times\vec{V}\right) + \kappa(\vec{\nabla}\times\vec{N}) + \vec{J}\times\vec{B}. \tag{2}$$

Conservation of angular momentum (micro-rotation):

$$\rho(\vec{N}.\vec{\nabla})\vec{N} = \gamma\vec{\nabla}(\vec{\nabla}.\vec{N}) + \kappa\left(\vec{\nabla}\times\vec{V}\right) - \gamma\vec{\nabla}\times\left(\vec{\nabla}\times\vec{N}\right) - 2\kappa\vec{N}. \tag{3}$$

Current density vector:

$$\vec{J} = \sigma(\vec{E} + \vec{V}\times\vec{B}) - \frac{\omega_e\tau_e}{B}\left(\vec{J}\times\vec{B}\right) + \frac{\omega_e\tau_e\omega_i\tau_i}{B^2}\left(\vec{J}\times\vec{B}\right)\times\vec{B}. \tag{4}$$

Maxwell's equations:

$$div\,\vec{B} = 0 \tag{5a}$$

$$\vec{\nabla}\times\vec{H} = \vec{J} \tag{5b}$$

$$\vec{\nabla}\times\vec{E} = 0. \tag{5c}$$

Energy equation:

$$\rho C_p(\vec{V}.\vec{\nabla})T = k\nabla^2 T + \Theta. \tag{6}$$

Θ is energy loss function due to viscosity and Joule heating.

To simplify the problem the authors assume that there is no variation of flow and heat transfer quantities in the z-direction as discussed by Rosenhead [25]. The equation of conservation of electric charge $\Delta.J = 0$ gives $J_y =$ constant. Since the wedge is non-conducting, $J_y = 0$, everywhere in the flow. Also, $E_x = 0$ and $E_z = 0$ everywhere in the fluid. The authors assumed that the induced magnetic field can be neglected in comparison to the applied magnetic field, but the viscous dissipation and Joule heating effects in the fluid are taken into account.

Under these assumptions the simplified equations in the Cartesian system are:

Conservation of mass:

$$\frac{\partial u}{\partial x} + \frac{\partial v}{\partial y} = 0. \tag{7}$$

Conservation of translational momentum:

$$u\frac{\partial u}{\partial x} + v\frac{\partial u}{\partial y} = \left(\frac{\mu+\kappa}{\rho}\right)\frac{\partial^2 u}{\partial y^2} + \frac{\kappa}{\rho}\frac{\partial N}{\partial y} + \frac{1}{\rho}\left[\frac{\sigma B_y^2}{\left(\alpha_e^2+\beta_e^2\right)}\left\{\alpha_e(U-u) - \beta_e w\right\}\right] + U\frac{dU}{dx} \tag{8}$$

$$u\frac{\partial w}{\partial x} + v\frac{\partial w}{\partial y} = \left(\frac{\mu+\kappa}{\rho}\right)\frac{\partial^2 w}{\partial y^2} - \frac{1}{\rho}\frac{\sigma B_y^2}{\left(\alpha_e^2+\beta_e^2\right)}\left(\alpha_e w - \beta_e u\right). \tag{9}$$

Conservation of angular momentum (micro-rotation):

$$\rho j\left(u\frac{\partial N}{\partial x} + v\frac{\partial N}{\partial y}\right) = \frac{\partial}{\partial y}\left(\gamma\frac{\partial N}{\partial y}\right) - \kappa\left(2N + \frac{\partial u}{\partial y}\right). \tag{10}$$

Conservation of energy:

$$\rho C_p\left(u\frac{\partial T}{\partial x} + v\frac{\partial T}{\partial y}\right) = k\frac{\partial^2 T}{\partial y^2} + (\mu+\kappa) \times\left[\left(\frac{\partial u}{\partial y}\right)^2 + \left(\frac{\partial w}{\partial y}\right)^2\right] + \frac{\sigma B_y^2}{\left(\alpha_e^2+\beta_e^2\right)}\left(u^2+w^2\right) \tag{11}$$

where, $\alpha_e = 1+\beta_i\beta_e$ and (u, v, w) are the velocity components along (x, y, z) directions

The boundary conditions for the flow are:

$$u = v = w = 0 \quad \text{and} \quad N = -n\frac{\partial u}{\partial y} \quad \text{and} \quad q_w = -k\frac{\partial T}{\partial y} \quad \text{at } y = 0, \tag{12}$$

$$u \to U, \qquad w \to 0, \qquad N \to 0 \quad \text{and} \quad T \to T_\infty \text{ as } y \to \infty. \tag{13}$$

Following [12], the authors assume that the free stream velocity is $U = ax^m$, where $m = \beta/(2-\beta)$, and β corresponds to $\beta = \Omega/\pi$ for angle Ω of the wedge, and a is a positive constant. As discussed by [23], the authors assume that $B_y = B_0 x^{\left(\frac{m-1}{2}\right)}$, where $0 \le m \le 1$ with $m = 0$ for the boundary layer flow over a stationary flat plate and $m = 1$ for the flow near the stagnation point on an infinite wall. In the boundary conditions "n" is a constant such that $0 \le n \le 1$. In the case when $n = 0$ is called strong concentration, which indicates $N = 0$ near the wedge, this represents concentrated particle flow where the micro-elements close to the wedge surface are unable to rotate (see Jena et al., 1981). In the case when $n = 1/2$, this indicates

the vanishing of the anti-symmetric part of the stress tensor and denotes weak concentration, whereas $n = 1$ is used for the modeling of turbulent boundary layer flow. Here the authors took the case of $n = 1/2$. It is known that $\gamma = (\mu + \kappa/2)\, j = \mu\,(1 + K/2)\, j$, where $K = \kappa/\mu$ is the dimensionless viscosity ratio and is called a material parameter.

The authors introduce the following similarity variables:

$$\psi = f(\eta)\left(\frac{2\nu x U}{m+1}\right)^{-1/2},$$

$$N = Uh(\eta)\left[\frac{(m+1)\,U}{2\nu x}\right]^{-1/2}, \qquad w = Ug(\eta)$$

$$\eta = \left[\frac{(m+1)\,U}{2\nu x}\right]^{-1/2} y,$$

$$\theta(\eta) = \frac{k(T - T_\infty)}{q_w}\left[\frac{(m+1)\,U}{2\nu x}\right]^{-1/2}, \qquad M = \frac{2\sigma B_0^2}{a\rho\,(m+1)}.$$

Eqs. (7)–(10) along with boundary conditions (1)–(4) reduce to:

$$(1+K)f''' + ff'' + \left(\frac{2m}{m+1}\right)\left(1 - f'^2\right) + Kh' + \frac{M}{\left(\alpha_e^2 + \beta_e^2\right)}\left[\alpha_e\left(1 - f'\right) - \beta_e g\right] = 0 \tag{14}$$

$$(1+K)g'' + g'f - \left(\frac{2m}{m+1}\right)gf' - \frac{M}{\left(\alpha_e^2 + \beta_e^2\right)}\left(\alpha_e g - \beta_e f'\right) = 0 \tag{15}$$

$$\left(1 + \frac{K}{2}\right)h'' - \left[\left(\frac{3m-1}{m+1}\right)hf' - fh'\right] - \frac{2K.I}{m+1}\left(2h + f''\right) = 0 \tag{16}$$

$$\frac{1}{\Pr}\theta'' + (m+1)f\theta' + \left[(m-1)f' + (1+K)\,Ec \times \left(f''^2 + g'^2\right) + \frac{Ec.M}{\left(\alpha_e^2 + \beta_e^2\right)}\left(f'^2 + g^2\right)\right]\theta = 0 \tag{17}$$

where, $(')$ represents the derivative with respect to η, ψ is steam function. i.e. $u = \frac{\partial\psi}{\partial y}$ and $v = -\left(\frac{\partial\psi}{\partial x}\right)$, $B = \frac{\nu^2 Re}{JU^2}$, $Ec = \frac{U^2}{C_p(T - T_\infty)}$ (Eckert number) and $\Pr = \frac{\mu C_p}{k}$ (Prandtl number).

Boundary conditions in non dimensional form are:

$$f(0) = 0, \qquad f'(0) = 0, \qquad g(0) = 0, \qquad h(0) = -\frac{1}{2}f''(0), \qquad \theta'(0) = -1 \tag{18}$$

$$f'(\infty) \to 1, \qquad g(\infty) \to 0, \qquad h(\infty) \to 0, \qquad \theta(\infty) \to 0. \tag{19}$$

The quantities of physical interest are local skin friction coefficients (C_{fx} and C_{fz}), local Nusselt number (Nu) and wall couple stress (C_r), which are defined as:

$C_{fx} = \frac{\tau_w}{\frac{1}{2}\rho U^2}$, $C_{fz} = \frac{\tau_z}{\frac{1}{2}\rho U^2}$, and $Nu = \frac{xq_w}{k(T - T_\infty)}$ respectively, where $\tau_w = \left[(\mu + \kappa)\frac{\partial u}{\partial y} + \kappa N\right]_{y=0}$, $\tau_z = \left[(\mu + \kappa)\frac{\partial w}{\partial y}\right]_{y=0}$, $q_w = -k\frac{\partial T}{\partial y}$ and $Re = \frac{Ux}{\nu}$.

Table 1: Values of $\frac{1}{2}C_{fx}Re^{1/2}$ for various values of K, M and m at $I = 0.5$, $\beta_i = 0.4$, $\beta_e = 0$ and $Ec = 0$.

K	M	m	[14]	[15]	[23]	Present result
0	0	0	0.332057	0.332206	0.3321	0.3466
0	0	1/3	0.757448	0.757586	0.7575	0.7586
0	0	1	1.232588	1.232710	1.2326	1.2328

Table 2: Values of $Nu \cdot Re^1/2$ for various values of Pr at $I = 0.5$, $\beta_i = 0.4$, $\beta_e = 0$ and $Ec = 0$.

K	M	m	Ec	Pr	[9]	[23]	Present result
0	0	0	0	1	0.45897	0.4590	0.460439
0	0	0	0	10	0.99789	0.9980	1.00012
0	0	0	0	100	2.15197	2.1520	2.163009
0	0	0	0	1000	4.63674	4.6367	4.647032
0	0	0	0	10000	9.98965	9.9897	10.00013
0	0	0	0.1	1	–	–	0.458130
0	0	0	0.5	1	–	–	0.419986

Therefore $C_{fx} = \sqrt{\frac{2(m+1)}{Re}}\left(1 + \frac{K}{2}\right)f''(0)$, $C_{fz} = \sqrt{\frac{2(m+1)}{Re}}(1+K)\,g'(0)$ and $Nu = \sqrt{\frac{(m+1)Re}{2}}\frac{1}{\theta(0)}$ respectively.

3. Method of solution

The non-linear ordinary differential equations (14)–(17) subjected to boundary conditions (18) and (19) have been solved using the Runge–Kutta Fehlberg method along with the shooting method. This method is based on the discretization of the problem domain and the calculation of unknown boundary conditions.

The domain of the problem is discretized and the boundary conditions for $\eta = \infty$ are replaced by $f'(\eta_{\max}) = 1$, $g(\eta_{\max}) = 1$, $h(\eta_{\max}) = 1$ and $\theta(\eta_{\max}) = 0$, where $\eta_{\max}$ is a sufficiently large value of η (corresponding to step size) at which the boundary conditions (19) for $f(\eta)$ are satisfied. The authors ran the computer code written in MATLAB for different values of $\eta_{\max}$ and for different values of step size $\Delta\eta$. They found that there is no, or only a negligible, change in the quantities of physical interest like Nusselt number and skin friction coefficients for values of η greater than 3. Also, after $\eta = 3$ the temperature is always zero. This means the numerical scheme is consistent and stable. Therefore, in the present work the authors have set $\eta_{\max} = 3.0$ and step size $\Delta\eta = 0.001$ taking into account the consistency and stability criteria. To solve the problem the non-linear equation (14)–(17) have been first converted into nine first order linear ordinary differential equations. There are five conditions at boundary $\eta = 0$ (values of the function) and four conditions at boundary $\eta = \infty$. To get the solution of the problem, one will need four more conditions at $\eta = 0$. These conditions have been found by the shooting technique. Finally the problem has been solved by the Runge–Kutta Fehlberg method along with calculated boundary conditions.

4. Results and discussion

In order to analyze the effects of various physical parameters on the flow, a numerical computation has been performed. To validate the results, the authors have compared the results with published work [9,14,15,23]. These comparisons are given in Tables 1 and 2. These results show that our resuts are in very good agreement with previously published work. The

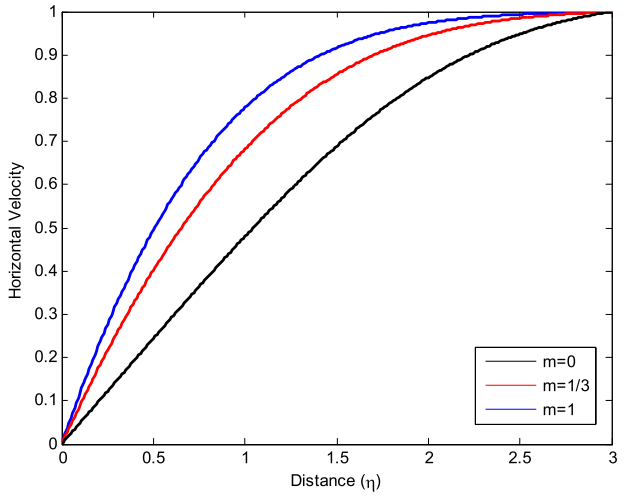

Figure 2: Horizontal Velocity Profile $f'(\eta)$ for different values of m when $K = 0$, $M = 0$, $\beta_e = 0$, $\beta_i = 0.4$, $I = Ec = 0.5$ and $Pr = 1$.

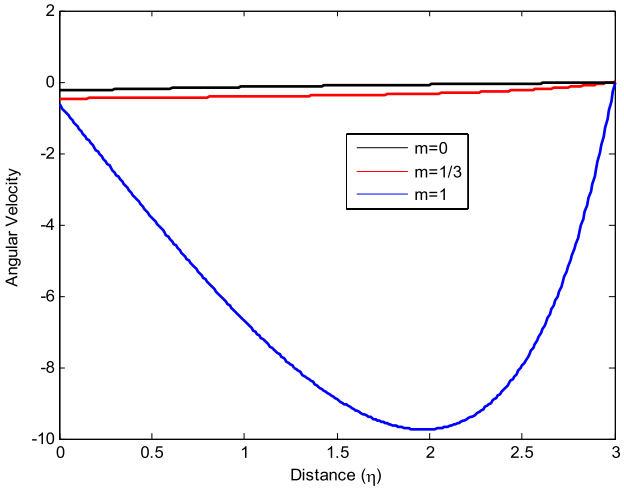

Figure 3: Angular Velocity Profile $h(\eta)$ for different values of m when $K = 0$, $M = 0$, $\beta_e = 0$, $\beta_i = 0.4$, $I = Ec = 0.5$ and $Pr = 1$.

effects of various physical parameters on horizontal velocity, transverse velocity, angular velocity profiles and temperature distribution have been discussed and shown in Figures 2–18. The effects of all these parameters on local skin friction coefficients (due to horizontal velocity as well as transverse velocity) and local Nusselt number have been given in Tables 1–5.

The effect of m or Ω (the angle of wedge) on velocity profiles and temperature distribution are shown in Figures 2–4. It is depicted from Figure 2, that the horizontal velocity $f'(\eta)$ increases with m and the momentum boundary layer thickness decreases. This in turn increases the velocity gradient at the surface ($\eta = 0$) and hence increases the skin friction coefficient. The skin friction coefficient for $m = 1$ is largest. Thus, the skin friction coefficient near the stagnation point of a plate is largest in comparison to the flow past a horizontal plate ($m = 0$) and the flow past a wedge ($0 < m < 1$). This results in an increase in local Nusselt number as given in Table 3.

Figure 3 shows that as we move away from the surface of the wedge the absolute value of angular velocity $|h(\eta)|$ decreases continuously for small values of m. i.e. for $m = 0$ and $m = 1/3$ (wedge angle 90°). In case of $m = 1$, the absolute value of

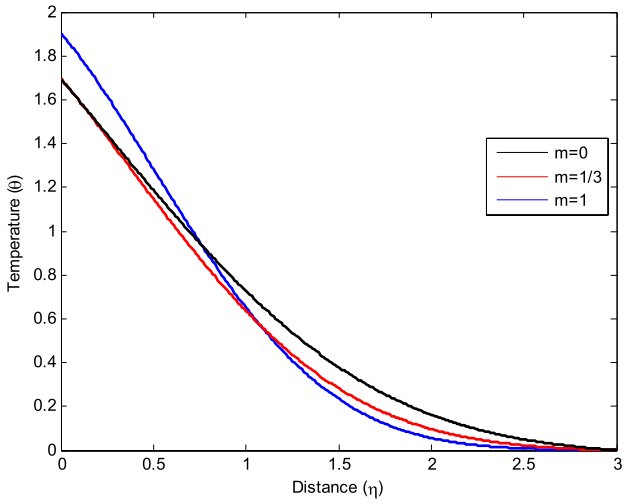

Figure 4: Temperature distribution $\theta(\eta)$ for different values of m when $K = 0$, $M = 0$, $\beta_e = 0$, $\beta_i = 0.4$, $I = Ec = 0.5$ and $Pr = 1$.

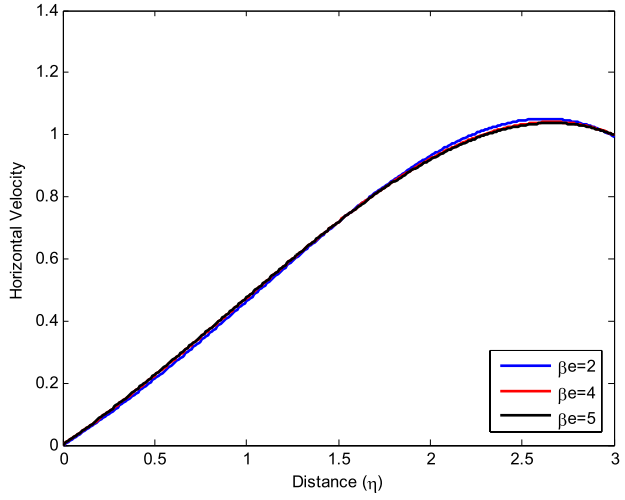

Figure 5: Horizontal Velocity $f'(\eta)$ for different values of β_e when $K = 1$, $M = 1$, $m = 1/3$, $\beta_i = 0.4$, $I = 0.5$, $Ec = 0.5$ and $Pr = 1$.

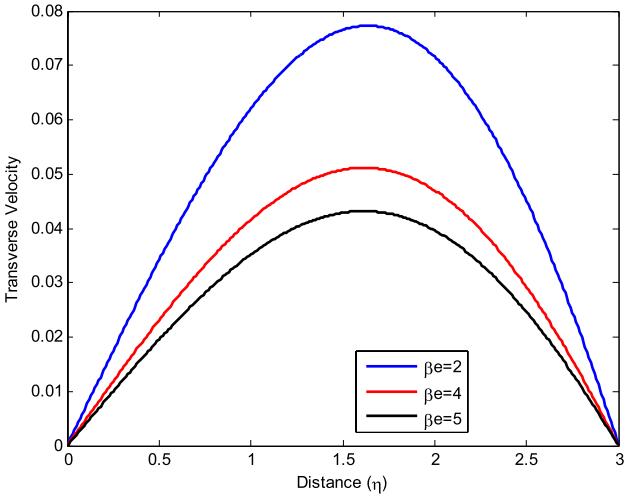

Figure 6: Transverse Velocity $g(\eta)$ for different values of β_e when $K = 1$, $M = 1$, $m = 1/3$, $\beta_i = 0.4$, $I = 0.5$, $Ec = 0.5$ and $Pr = 1$.

Table 3: Values of $1/2C_{fx}Re^{1}/2$, $1/2C_{fz}Re^{1}/2$ and $Nu.Re^{-1/2}$ for various values of m and M.

$I = 0.5, \beta_i = 0.4, \beta_e = 0, M = 0, K = 0, Pr = 1$ and $Ec = 0.5$				$M = 1, m = 1/3, \beta_i = 0.4, \beta_e = 2, I = 0.5, Pr = 1$ and $Ec = 0.5$			
m	$\frac{1}{2}C_{fx}Re^{1/2}$	$Nu.Re^{-1/2}$	$\frac{1}{2}C_{fz}Re^{1/2}$	K	$\frac{1}{2}C_{fx}Re^{1/2}$	$Nu.Re^{-1/2}$	$\frac{1}{2}C_{fz}Re^{1/2}$
0	0.3466	0.4200	–	0	0.8425	0.4726	0.1225
1/3	0.7586	0.4845	–	0.5	0.8386	0.4244	0.1295
1	1.2328	0.5297	–	1	0.4672	0.3999	0.1150

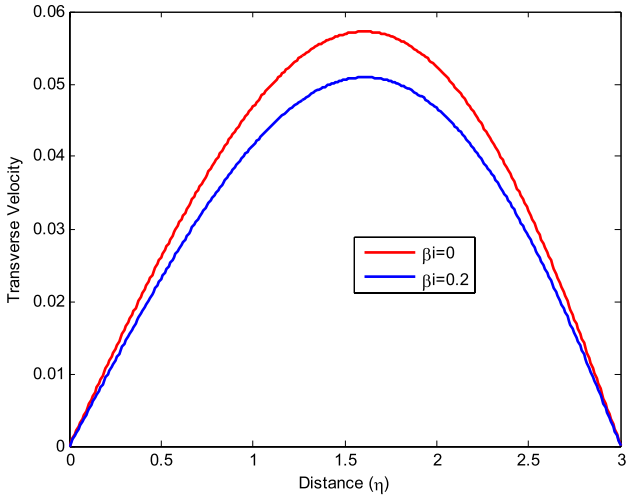

Figure 7: Transverse Velocity $g(\eta)$ for different values of β_i when $K = 1$, $M = 1, m = 1/3, \beta_e = 5, I = 0.5, Ec = 0.5$ and $Pr = 1$.

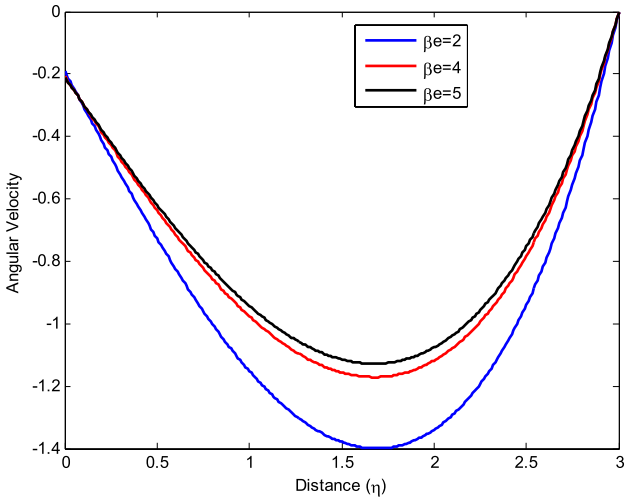

Figure 9: Angular Velocity $h(\eta)$ for different values of β_e when $K = 1, M = 1$, $m = 1/3, \beta_i = 0.4, I = 0.5, Ec = 0.5$ and $Pr = 1$.

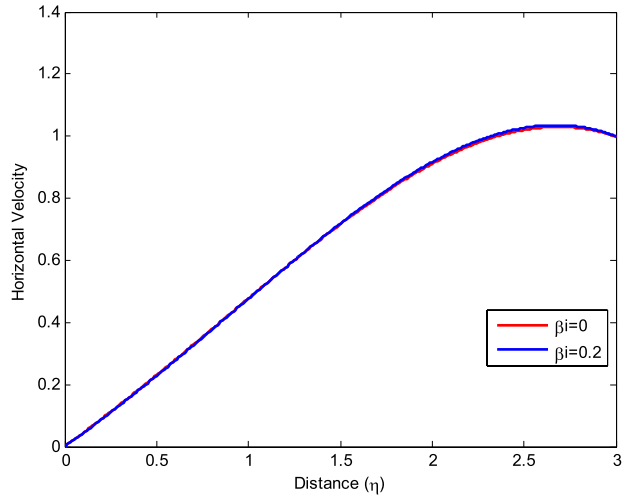

Figure 8: Horizontal Velocity Profile for different values of β_i when $K = 1$, $M = 1, m = 1/3, \beta_e = 5, I = 0.5, Ec = 0.5$ and $Pr = 1$.

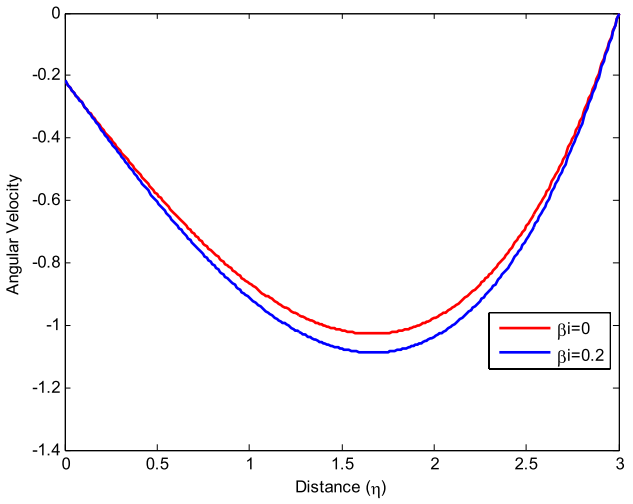

Figure 10: Angular Velocity Profile for different values of β_i when $K = 1$, $M = 1, m = 1/3, \beta_e = 5, I = 0.5, Ec = 0.5$ and $Pr = 1$.

angular velocity first increases, but after a certain distance from the surface of the wedge it decreases. This figure also shows that the gradient of angular velocity near the surface increases with the increase in m and thus the shear stress increases with the increase in the angle of wedge.

Figure 4 depicts the effect of m on temperature distribution. The value of temperature at the surface increases slightly with the increase in the value of m, but at $m = 1$ it increases rapidly. However, as we move away from the surface the effect is just reversed. i.e. temperature decreases with the increase in m from 0 to 1. From the graph it is also clear that, the thermal boundary layer thickness decreases with the increase in m. Thus the heat transfer rate for the wedge with large angles is higher.

Figures 5–8 depict the effect of β_e and β_i on velocities and temperature distribution. Figure 5 depicts that with the increase in β_e horizontal velocity $f'(\eta)$ increases slightly near the surface of the wedge, but after a certain distance it decreases. This means the Hall current at the surface of the wedge enhances the fluid velocity slightly. This is because of the increase in Lorentz force near the surface of the wedge. This increases the velocity gradient near the wall and results in an increase in local skin friction coefficient $C_{fx}Re^{1/2}$.

The values of skin friction coefficients for various values of β_e and β_i are given in Table 4. The effect of Hall current and ion slip on the transverse component of velocity is shown in Figures 6 and 7. Due to the increase in Hall and ion slip currents, the force

Table 4: Values of $1/2C_{fx}Re^{1}/2$, $1/2C_{fz}Re^{1}/2$ and $Nu.Re^{-1/2}$ for various values of β_e and β_i.

$M=1, m=1/3, \beta_i=0.4, K=1, I=0.5, Pr=1$ and $Ec=0.5$				$M=1, m=1/3, \beta_e=5, I=0.5, K=1, Pr=1$ and $Ec=0.5$			
β_e	$\frac{1}{2}C_{fx}Re^{1/2}$	$Nu.Re^{-1/2}$	$\frac{1}{2}C_{fz}Re^{1/2}$	β_i	$\frac{1}{2}C_{fx}Re^{1/2}$	$Nu.Re^{-1/2}$	$\frac{1}{2}C_{fz}Re^{1/2}$
2	0.4672	0.3999	0.1150	0	0.5330	0.4055	0.0882
4	0.5090	0.4050	0.0799	0.2	0.5233	0.4056	0.0781
5	0.5162	0.4058	0.0660	0.4	0.5162	0.4058	0.0660

Table 5: Values of $1/2C_{fx}Re^{1}/2$, $1/2C_{fz}Re^{1}/2$ and $Nu.Re^{-1/2}$ for various values of M and B.

$I=0.5, \beta_i=0.4, \beta_e=5, m=1/3, K=1, Pr=1$ and $Ec=0.5$				$M=1, m=1/3, \beta_i=0.4, \beta_e=2, K=1, Pr=1$ and $Ec=0.5$			
M	$\frac{1}{2}C_{fx}Re^{1/2}$	$Nu.Re^{-1/2}$	$\frac{1}{2}C_{fz}Re^{1/2}$	I	$\frac{1}{2}C_{fx}Re^{1/2}$	$Nu.Re^{-1/2}$	$\frac{1}{2}C_{fz}Re^{1/2}$
0.5	0.5286	0.4070	0.0336	0.5	0.4672	0.3999	0.1150
2	0.4937	0.4027	0.1266	2	1.0672	0.3636	0.1413
5	0.4473	0.3889	0.2779	4	1.0570	0.3675	0.1395

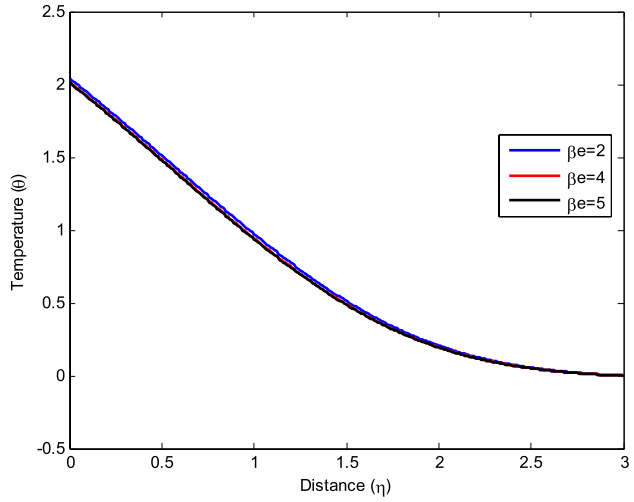

Figure 11: Temperature distribution for different values of β_e when $K = 1$, $M = 1, m = 1/3, \beta_i = 0.4, I = 0.5, Ec = 0.5$ and $Pr = 1$.

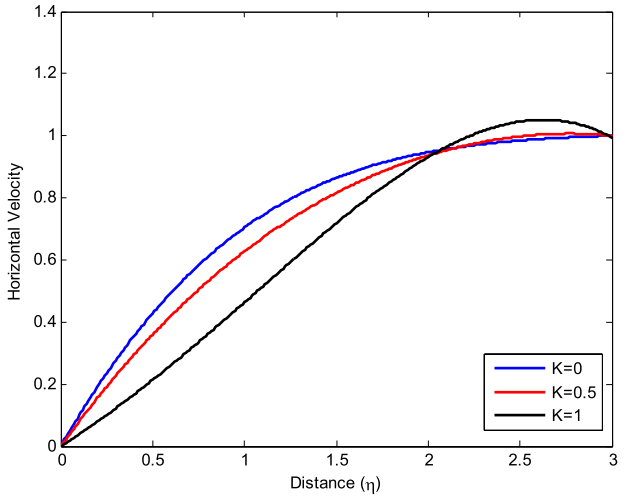

Figure 13: Horizontal Velocity Profile $f'(\eta)$ for different values of K when $M = 1, m = 1/3, \beta_e = 2, \beta_i = 0.4, I = 0.5, Ec = 0.5$ and $Pr = 1$.

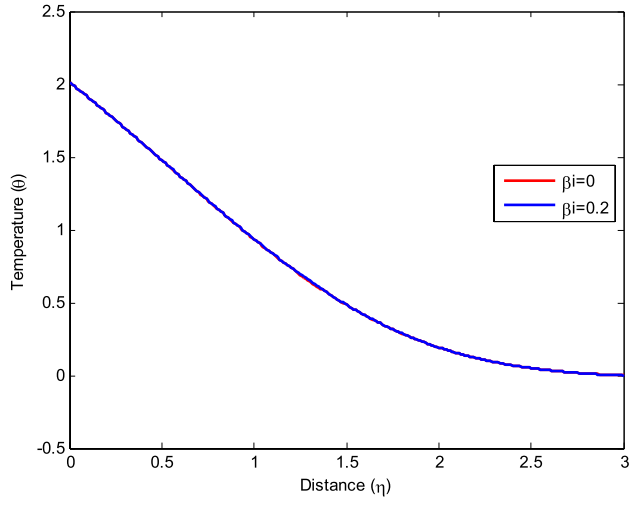

Figure 12: Temperature distribution $\theta(\eta)$ for different values of β_i when $K = 1$, $M = 1, m = 1/3, \beta e = 5, I = 0.5, Ec = 0.5$ and $Pr = 1$.

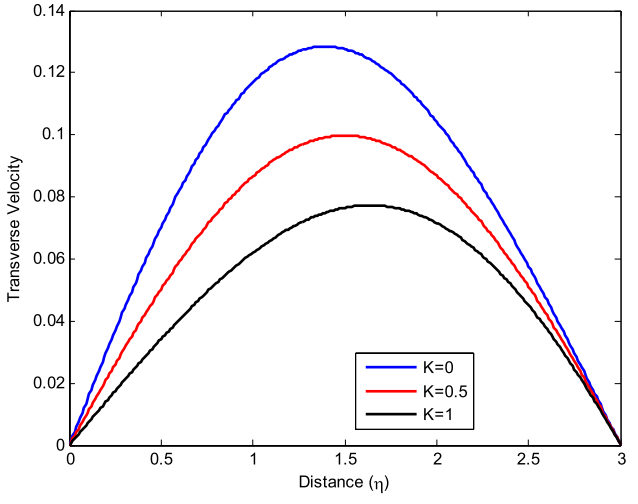

Figure 14: Transverse Velocity Profile $g(\eta)$ for different values of K when $M = 1, m = 1/3, \beta_e = 2, \beta_i = 0.4, I = 0.5, Ec = 0.5$ and $Pr = 1$.

in the direction of z-decreases, which caused the decrease in the transverse velocity of the fluid, as shown in Figures 6 and 7.

Since the magnitude of transverse velocity component is very small, there is a very small increase in the horizontal velocity component with the change in β_i. This effect of ion slip on the horizontal velocity profile is shown in Figure 8, and from Table 4 it is observed that there is a slight decrease in the value of local skin friction coefficient $C_{fx}Re^{1/2}$ with the increase in β_i.

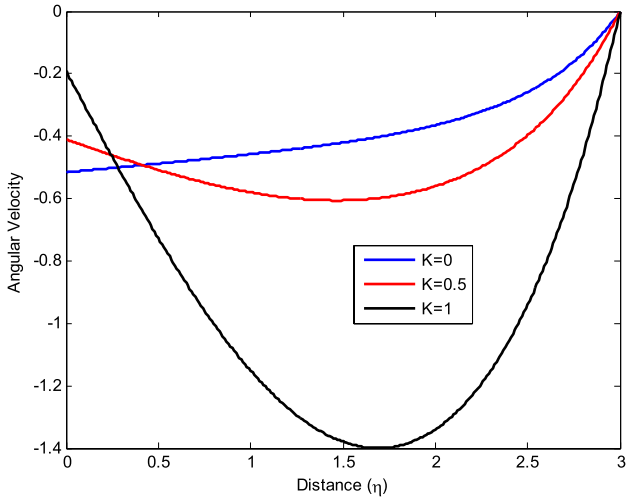

Figure 15: Angular Velocity Profile $h(\eta)$ for different values of K when $M = 1$, $m = 1/3$, $\beta_e = 2$, $\beta_i = 0.4$, $I = 0.5$, $Ec = 0.5$ and $Pr = 1$.

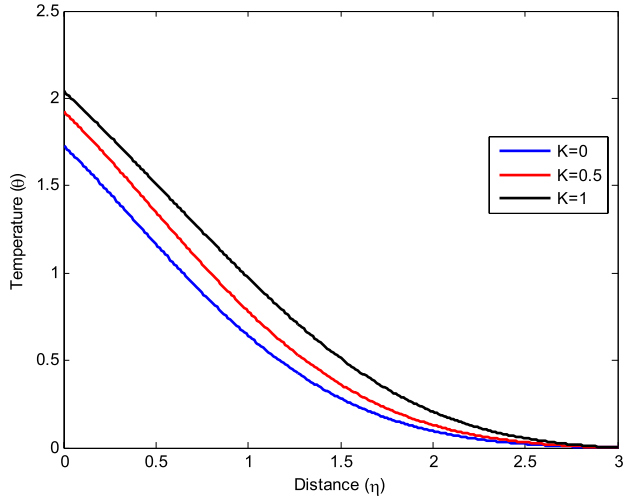

Figure 16: Temperature Distribution $\theta(\eta)$ for different values of K when $M = 1$, $m = 1/3$, $\beta_e = 2$, $\beta_i = 0.4$, $I = 0.5$, $Ec = 0.5$ and $Pr = 1$.

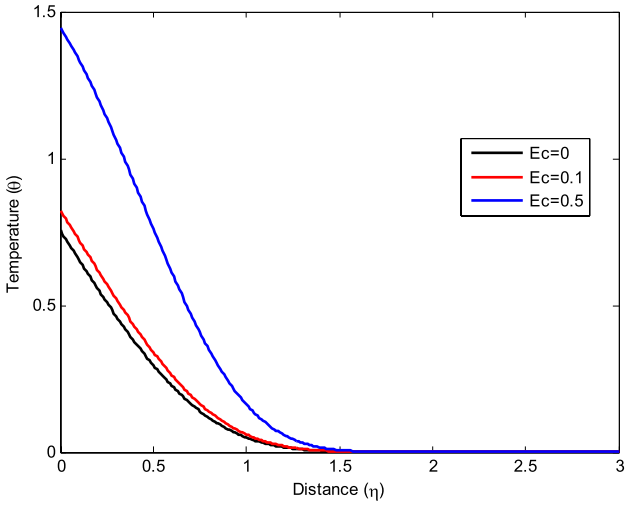

Figure 17: Temperature Distribution $\theta(\eta)$ for different values of Ec when $K = 1$, $M = 1$, $m = 1/3$, $\beta_e = 2$, $\beta_i = 0.4$, $I = 0.5$ and $Pr = 10$.

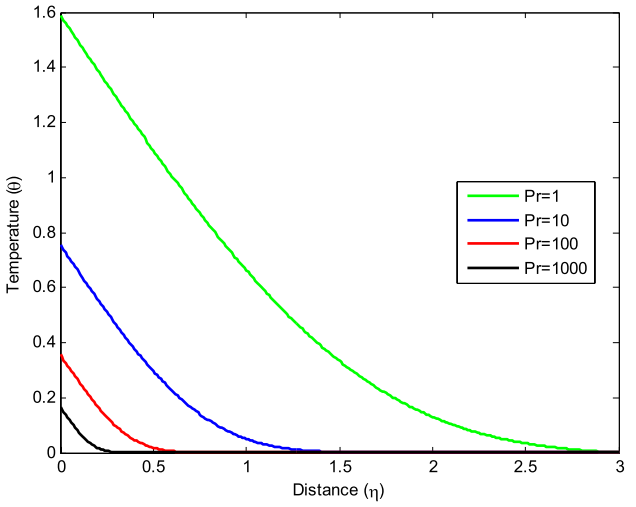

Figure 18: Temperature Distribution $\theta(\eta)$ for different values of Pr when $K = 1$, $M = 1$, $m = 1/3$, $\beta_e = 2$, $\beta_i = 0.4$, $I = 0.5$ and $Ec = 0$.

The angular velocity of the particles in fluid depends upon the velocity of the fluid. Therefore, the effect of Hall currents directly affects the angular velocity of the particles. Since the transverse velocity of the fluid decreases with the increase in Hall current, the angular velocity of the particles increases in the opposite direction. From Figure 9, it is observed that the angular velocity of the particles increases in opposite direction to the increase in Hall current, i.e. the magnitude of angular velocity decreases with the increase in β_e. This causes the decrease in angular velocity gradient near the wall and, results in decreased wall couple stress. Figure 10 shows that the magnitude of angular velocity increases with the increase in β_i which therefore increases wall couple stress.

It is clear from Figures 11 and 12 that the temperature decreases slightly with the increase in β_e while there is no effect of ion slip parameter on the temperature. The temperature distribution in the fluid depends upon the stream of fluid and the velocity gradients of the fluid. In the present case, the change in horizontal velocity is very small or negligible with the change in β_e and β_i. Therefore, the change in temperature mainly depends upon the transverse velocity. The decrease in transverse velocity with the increase in β_e and β_i causes the decrease in temperature. But the value of transverse velocity is very small. Therefore, there is a small change in temperature with the increase in β_e and a negligible change with the increase in β_i. This effect of β_e and β_i concludes that the local Nusselt number i.e. heat transfer rate increases slightly with the increase in β_e, but there is no effect of β_i on the Nusselt number, as given in Table 4.

The increase in the vortex viscosity (κ) of fluid particles increases the overall viscosity of the fluid. Thus, the increase in material parameter K ($K = \kappa/\mu$ dimensionless viscosity ratio), simply implies the increase in the resultant viscosity of the fluid. With the increase in material parameter K ($K = \kappa/\mu$ dimensionless viscosity ratio), horizontal velocity decreases and after a fixed distance away from the surface it increases. It shows that the effect of vortex viscosity near the surface of the wedge is greater as compared to its effect in free stream. The transverse velocity shows a uniform decreasing pattern with the increase in the value of K as depicted in Figures 13 and 14. It is also clear from the figures that the velocity gradients

near the surface decrease, hence producing a decrease in skin friction coefficient. Thus micropolar fluids show a reduction in local skin drag as compared to Newtonian fluids. The numerical values of skin friction coefficients for various values of K are given in Table 3.

The effect of vortex viscosity is greater near the surface of the wedge as compared to the free stream. Therefore, the absolute value of angular velocity near the surface decreases with the increase in the value of material parameter, and as we move away from the wedge this value increases as depicted in Figure 15. These changes result an increase in the rotation of the particles near the surface and hence an increase in wall couple stress. Thus the increase in material parameter is to accelerate the particle rotation near the surface.

The increased material parameter increases the resultant viscosity of the fluid and generates more heat due to the increased viscous forces. Therefore, the temperature as well as thermal boundary layer thickness increases with the increasing value of K as seen in Figure 16. Due to the increased temperature and thickening of thermal boundary layer, the local Nusselt number decreases with the increasing value of material parameter. The variation of Nusselt number is shown in Table 4. This table also signifies that an increase in skin friction, increases the heat transfer rate.

Physically the Eckert number (**Ec**) is the measure of viscous dissipation. Therefore, increasing the value of Ec implies more dissipation, i.e. an increase in the temperature of the fluid. Figure 17 depicts that the temperature at the surface of the wedge, as well as the thermal boundary layer thickness increases with the increase in Ec. This causes a decrease in heat transfer rate.

Figure 18 shows that increasing the value of Prandtl number (**Pr**) decreases the thermal boundary layer thickness and results in a decreasing heat transfer rate. This effect is very obvious from the physical meaning of Pr, i.e. the ratio of kinematic viscosity to thermal. These variations are also presented in Table 2.

The effects of other parameters on local skin friction coefficients and local Nusselt number are given in Table 5. From this table it is concluded that the increasing value of magnetic field M decreases skin friction coefficients and increases heat transfer rate. Further, the inertial parameter shows an increase in skin friction coefficients upto a fixed value of the parameter, but after this value the trend gets reversed. Similarly the local Nusselt number decreases with the increase in material parameter, but after the same fixed value of the parameter it decreases.

5. Conclusions

The authors have theoretically studied the problem, and found the numerical results for local Nusselt number and local skin friction coefficients. They analyzed the effect of Hall and ion slip along with material properties, on the fluid flow behavior and heat transfer characteristics. From the results it is shown that the findings of the present problem are in very good agreement with previously published work, for some particular cases. From the numerical calculations of Nusselt number and skin friction coefficients it is concluded that in a micro polar fluid, the Hall effect enhances the heat transfer rate (Nusselt number) significantly, but there is a negligible effect of ion slip on heat transfer rate. On the other hand for particular values of Hall and ion slip parameters an increase in magnetic field decreases the heat transfer rate at the surface. It is also concluded that increasing magnetic field reduces skin friction coefficient due to the translational motion of the fluid whereas, it increase skin friction due to rotational motion. For a particular value of magnetic field, there is deterioration in the local skin friction coefficient due to the rotational motion of the fluid with the increase in Hall parameter as well as ion slip parameter. However, the effect is just opposite for the local skin friction coefficient due to translational motion. The authors also found that the heat transfer rate at the surface increase very fast with the increase in the value of Prandtl number (Pr), and there is no effect of Prandtl number on the skin friction coefficients in the present problem. Therefore, in heat transfer applications the micropolar fluid with high Prandtl number can be used. Therefore the authors concluded that the use of waste industrial fluid could be a good option for cooling applications with the same configuration as discussed in this paper. In future studies, the effect of radiation along with the case of heat generation/absorption will be considered for the heat transfer flow of micropolar fluids past wedge shaped bodies, and we will examine the ability of the perturbation method in solving problem.

References

[1] Eringen, A.C. "Theory of micropolar fluids", *J. Math. Mech.*, 16, pp. 1–18 (1966).
[2] Eringen, A.C. "Theory of thermomicropolar fluids", *J. Math. Anal. Appl.*, 38, pp. 480–496 (1972).
[3] Lukaszewicz, G., *Micropolar Fluids: Theory and Applications*, Basel Birkhauser (1999).
[4] Eringen, A.C., *Microcontinuum Field Theories. II, Fluent Media*, Springer, New York (2001).
[5] Jena, S.K. and Mathur, M.N. "Similarity solutions for laminar free convection flow of a thermomicropolar fluid past a non-isothermal vertical plate", *Int. J. Engng. Sci.*, 19(11), pp. 1431–1439 (1981).
[6] Beg, O.A., Bhargava, R., Rawat, S. and E, Kahya "Numerical study of micropolar convective heat and mass transfer in a non-Darcy porous regime with Soret and Dufour effects", *Emirates. J. Engng. Res.*, 13(2), pp. 51–66 (2008).
[7] Norfifah, B. and Ishak, A. "MHD stagnation point flow of a micropolar fluid with prescribed wall heat flux", *European. J. Sci. Res.*, 35(3), pp. 436–443 (2009).
[8] Pal, D. and Chatterjee, S. "Mixed convection magnetohydrodynamic heat and mass transfer past a stretching surface in a micropolar fluid-saturated porous medium under the influence of Ohmic heating, Soret and Dufour effects", *Commun. Nonlinear Sci. Numer. Simul.*, 16(3), pp. 1329–1346 (2011).
[9] Lin, H.T. and Lin, L.K. "Similarity solutions for laminar forced convection heat transfer from wedges to fluids of any Prandtl number", *Int. J. Heat Mass Transfer*, 30, pp. 1111–1118 (1987).
[10] Kim, Y.J. "Thermal boundary layer flow of a micropolar fluid past a wedge with constant wall temperature", *Acta Mech.*, 138, pp. 113–121 (1999).
[11] Kim, Y.J. and Kim, T.A. "Convective micropolar boundary layer flows over a wedge with constant surface heat flux", *Int. J. Appl. Mech. Engng.*, 8, pp. 147–153 (Special issue: ICER 2003) (2003).
[12] Falkner, V.M. and Skan, S.W. "Some approximate solutions of the boundary layer equations", *Philos Mag.*, 12, pp. 865–896 (1931).
[13] Kafoussias, N.G. and Nanousis, N.D. "Magnetohydrodynamic laminar boundary-layer flow over a wedge with suction or injection", *Can. J. Phys.*, 75, pp. 733–745 (1997).
[14] Yih, K.A. "MHD forced convection flow adjacent to a non-isothermal wedge", *Int. Comm. Heat Mass Transfer*, 26, pp. 819–827 (1999).
[15] Chamka, A.J., Mujtaba, M., Qadri, A. and Issa, C. "Thermal radiation effects on MHD forced convection flow adjacent to a non-isothermal wedge in the presence of heat source or sink", *Heat Mass Transfer*, 39, pp. 305–312 (2003).
[16] Param Jeet Singh,, Roy, S. and Ravindran, R. "Unsteady mixed convection flow over a vertical wedge", *Int. J. Heat Mass Transfer*, 52, pp. 415–421 (2008).
[17] Rashad, A.M. and Bakier, A.Y. "MHD Effects on Non-Darcy Forced convection boundary layer flow past a permeable wedge in a porous medium with uniform heat flux", *Nonlinear Anal. Model. Control*, 14(2), pp. 249–261 (2009).
[18] Seddeek, M.A. and Abdelmeguid, M.S. "Hall and Ion-slip effects on magneto-micropolar fluid with combined forced and free convection in boundary layer flow over a horizontal plate", *J. KSAIM*, 8(2), pp. 51–73 (2004).
[19] Hazem, Attia Ali. "Hall effect on Couettes flow with heat transfer of a dusty conducting fluid in the presence of uniform suction and injection", *Afr. J. Math. Phys.*, 2(1), pp. 97–110 (2005).
[20] Hazem, Attia Ali. "The effect of variable properties on the unsteady Couette flow with heat transfer considering the Hall effect", *Commun. Nonlinear Sci. Numer. Simul.*, 13, pp. 1596–1604 (2008).

[21] Ibrahim, A.Abdallah. ''Analytic solution of heat and mass transfer over a permeable stretching plate affected by chemical reaction, internal heating, Dufour–Soret effect and hall effect'', *Thermal Sci.*, 13(2), pp. 183–197 (2009).
[22] Elgazery, N.S. ''The effects of chemical reaction, hall and ion slip currents on MHD flow with temperature dependent viscosity and thermal diffusivity'', *Commun. Nonlinear Sci. Numer. Simul.*, 14, pp. 1267–1283 (2009).
[23] Ishak, A., Nazar, R. and Pop, I. ''MHD boundary-layer flow of a micropolar fluid past a wedge with constant wall heat flux'', *Commun. Nonlinear Sci. Numer. Simul.*, 14, pp. 109–118 (2009).
[24] Sutton, G.W. and Sherman, A., *Engineering Magnetohydrodynamics*, McGrawHill (1965).
[25] Rosenhead, L., *Laminar Boundary Layers*, Dover publications, Inc, New York (1963).

Ziya Uddin is Post Doctoral Researcher in the Université de Valenciennes et du Hainaut-Cambrésis, Valenciennes, France. He obtained his Ph.D. degree from G.B. Pant University of Agriculture and Technology, Pantnagar, India, and, subsequently, worked as Assistant Professor of Mathematics in India. His current research interests include: analytical and numerical solutions of nonlinear problems arising in applied sciences and engineering phenomena related to fluid flow and thermal systems.

Manoj Kumar obtained his Ph.D. degree from the University of Roorkee, India, and is, currently, Professor of Mathematics in the Department of Mathematics, Statistics and Computer Science at G.B. Pant University of Agriculture and Technology, Pantnagar, India. He has supervised many students at Ph.D. and M.S. degree levels. His current research interest mainly include: nonlinear science, industrial engineering and computational fluid mechanics.